East European Journal of Physics. 4. 607-619 (2025)
DOI:10.26565/2312-4334-2025-4-64 ISSN 2312-4334

SIMULATION OF FOCUSING A HOLLOW ELECTRON BEAM BY THE SYMMETRIC MAGNETIC LENS FOR INDUSTRIAL APPLICATION IN ADDITIVE TECHNOLOGIES

Igor V. Melnyk[1]*, Serhii B. Tuhai[1], Mykhailo Yu. Skrypka[1], Mykola S. Surzhikov[1], Oleksandr M. Kovalenko[1], Dmytro V. Kovalchuk[2]
[1]National Technical University of Ukraine "Igor Sikorsky Kyiv Polytechnical Institute", Kyiv, Ukraine
**Corresponding Author e-mail: imelnik@phbme.kpi.ua; Tel: 066-981-70-66*
[2]Joint Stock Company, Scientific and Industrial Association "Chervona Hvylia", Kyiv, Ukraine
Received July 22, 2025; revised November 11, 2025; in final form November 18, 2025; accepted November 20, 2025

The article studies the focusing features of a short-focus hollow electron beam formed from a wide surface of a cold cathode in high-voltage glow discharge electron guns using numerical simulation techniques. Such a type of electron beam is widely used today for producing new kinds of metals with unique properties by melting wire, which moves in a vertical direction through the ring-like beam focus. After that, the melted metal is crystallized on the horizontally moving substrate, which is located near the focus of the electron beam below. Such modern technology is considered three-dimensional printing of metal, or additive technologies. The original software created by the authors in the Python programming language has been used to obtain the corresponding simulation results. Analysis of the obtained numerical simulation results proved that with a small change in the beam trajectory divergence angle or the radius of the initial point on the cathode surface, the beam focus position, as a rule, does not change. Therefore, the annular focus of the beam is usually in a stable position on the longitudinal coordinate, and the thickness of the focal ring is always in the range of several millimeters. The corresponding theoretical results were compared with experimental data, and the difference between the theoretical and experimental results is in the range of 10-15% depending on the accelerating voltage and size of the cathode surface. High-voltage glow discharge electron guns with such parameters, by the thickness of the focal ring, can be successfully used in advanced industrial additive technologies for three-dimensional printing on metal surfaces by uniform heating along the perimeter of moving wires or rods with a variable diameter in the range of 0.5 – 10 mm.
Keywords: *Additive technologies; Electron beam technologies; Magnetic focusing; Hollow conical electron beam; Numerical simulation*
PACS: 29.25.Bx, 03.50.De

INTRODUCTION

Electron beam technologies are widely used in different branches of industry, especially in the technologies of additive production [1 – 16]. The special place in these technologies occupied the High-Voltage Glow Discharge Electron Guns (HVGDEG), which formed profile electron beams [15, 16]. It caused by such advanced particularities of HVGDEG, as relative simplicity of engineering construction, [17 – 29], operation with different active and noble technological gases [28, 29], as well as simplicity of control of Electron Beam (EB) current both aerodynamically by changing operation pressure in the gun chamber with controlled gas inlet and uninterrupted pumping [29] and electrically by changing the current of additional low-voltage gas discharge [30, 31]. Another advantage of HVGDEG is the possibility of forming EB with complex spatial geometry, including hollow conical EB with ring-like focus and ribbon electron EB with line focus. General approaches for estimating the geometry parameters of such types of HVGDEG are given in the papers [15, 16]. Generally, this possibility is explained by the relatively small current density from the cathode surface; therefore, enlarging the surface for forming a powerful EB is really necessary [28].

Today EB equipment is widely used in advanced technologies of additive production [1 – 16]. The main distinguishing features of additive technologies are significant savings in electricity and consumables, high equipment productivity, and, most importantly, the ability to obtain new ultra-high purity materials with unique properties. Therefore, the main areas of industry in which additive technologies are used today are the chemical industry, shipbuilding, aircraft manufacturing, and the space industry. Generally, lasers and EB as technological instruments, are used today in equipment for additive production. The process of laser heating can be realized in air; therefore, such equipment is usually cheaper [1 – 15]. But, on the contrary, the advantages of EB equipment are high productivity and high purity of production, as well as unique physical and chemical properties of obtained materials [15].

Expanded capabilities for designing electron-beam equipment in modern additive technologies, including the use of High-Voltage Glow Discharge Electron Guns (HVCDEG), which form a hollow conical EB [15, 16]. The main advantage of using this type of gun in the implementation of additive technologies with wire melting directly near the substrate is that the hollow conical electron beam uniformly heats the wire along its entire perimeter [15, 16].

It should be pointed out that there are two possible ways to form the hollow conical EB in HVGDEG, namely, using electrostatic focusing with cathode geometry as part of a sphere [15] and focusing in a short magnetic lens with the plane cathode geometry [16]. The basic structure scheme of HVGDEG construction with electrostatic focusing with cathode geometry as part of a sphere is presented in Fig. 1 [16]. The main advantage of this construction is the stable position of

Cite as: I.V. Melnyk, S.B. Tuhai, M.Yu. Skrypka, M.S. Surzhikov, O.M. Kovalenko, D.V. Kovalchuk, East Eur. J. Phys. 4, 607 (2025), https://doi.org/10.26565/2312-4334-2025-4-64

the electron beam focus, simplicity of the focusing systems, as well as the relatively stable focal current density throughout the whole time of providing the technological process. But, on the contrary, HVGDEG electrode systems with electrostatic focusing are difficult to exploit and assemble. Corresponding recommendations on parameters of HVGDEG from the point of view of the coaxial arrangement of gun parts have been considered in papers [15]. Changing the diameter of EB focal ring, as well as its thickness, for different wire diameters in such construction, is also impossible without changing the electrode system.

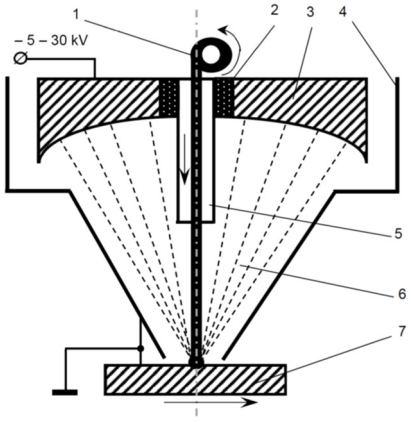

Figure 1. Generalized constructive scheme of HVGDEG with spherical cathode for three-dimensional printing by metal. 1 – moving ware, 2 – high-voltage insulator, 3 – cathode of HVGDEG, 4 – anode of HVGDEG, 5 – wire feed mechanism, 6 – hollow conical EB, 7 – moving substrate

Therefore, the aim of this paper is estimation of trajectories of hollow conical EB, which is formed from the cathode with plane geometry by focusing in a short magnetic lens [16]. It is clear that the main advances of this HVGDEG electrode system are the possibility of changing the diameter of the focal ring of the hollow EB and its thickness [16]. For providing these researches, the original computer software [32–34], created in the Python programming language [35-37], has been used.

STATEMENT OF SIMULATION PROBLEM AND MODEL PARAMETERS

The basic structure scheme of HVGDEG construction with plane cathode geometry and magnetic lens for focusing of hollow EB is presented in Fig. 2 [16].

From the point of view of the fundamental laws of electron optics [38–42], it is well known that only a diverging electron beam can be focused in the magnetic field of a short-focus lens. Since the cathode surface is flat, the divergence of electrons in the initial section of the trajectory near the cathode is caused by their dissipation on the atoms of the residual gas, in accordance with the Rutherford model [39, 41–45]. As for the defocusing of the beam by the intrinsic space charge of the electrons, under the physical conditions of a high-voltage glow discharge (HVGD), it is absent, since it is compensated for by the space charge of the positive ions of the residual gas [43–45].

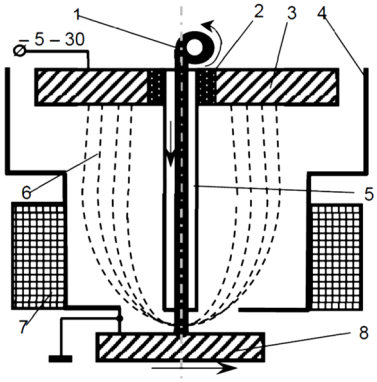

Figure 2. Generalized constructive scheme of HVGDEG with plane cathode and focusing magnetic lens for three-dimensional printing by metal. 1 – moving ware, 2 – high-voltage insulator, 3 – cathode of HVGDEG, 4 – anode of HVGDEG, 5 – wire feed mechanism, 6 – hollow EB, 7 – focusing magnetic lens, 8 – moving substrate

Another important property of HVGD electrode systems is the presence of anode plasma (AP) in the near-anode region. AP always has a clearly defined boundary. Therefore, in numerical modeling problems, it is usually considered as a source of ions' flow and as an electrode with a fixed potential transparent for the electron beam [28, 31]. The anode plasma (AP) region in HVGD photographs is always separated from the region of charged particle acceleration in the electric field, which is usually called the cathode fall region (CFR). Indeed, the AP is always the brighter part of the HVGD combustion region image [28, 31].

In general, from a physical point of view, in theoretical estimates, the AP boundary is usually defined as a fraction of the volume it occupies in the electrode system under consideration. Therefore, the position of the AP boundary always depends significantly on the accelerating voltage and the type and pressure of the residual gas, as well as on the geometry of the electrodes, including a spherical or flat cathode and a hollow anode of the HVGD. The geometry of the AP boundary always changes with a change in the discharge current in accordance with the geometry of the hollow anode surface. With an increase in the HVGD current and the pressure in the volume where the discharge is ignited, the AP boundary moves asymptotically toward the cathode surface and, at high discharge currents, becomes geometrically similar to it [21–25]. A correct estimate of the position of the AP boundary in an electrode system with a flat cathode surface and a cylindrical hollow anode is given in [16].

If the above-described physical conditions of the HVGD combustion in the electrode system presented in Fig. 2 are taken into account, the input parameters of the statement simulation task are as follows.

1. Acceleration voltage U_c.
2. Operation pressure p_g, and, correspondently, current of EB I_b, which is usually defined by the current-voltage characteristic of HVGD [28].
3. Angle of beam divergence α near the cathode surface.
4. Maximal and minimal value of EB radius $r_{b_{\max}}$ and $r_{b_{\min}}$ in the region of AP boundary, there zone of free moving of electrons is started.
5. Start point on transversal coordinate z_{start}, which correspond to position of AP boundary.
6. Parameters of magnetic lens, including its current I_l, number of coils N_l, as well as necessary geometry parameters, corresponding to considered model for defining magnetic inductivity, which will be described later.

Output parameters of considered simulation task are as follows.

1. Position of focal beam ring F_b.
2. Radius of focal beam ring R_b.
3. Thickness of focal beam ring T_b.

Corresponding input and output geometry parameters of the hollow conical EB are clearly explained in Fig. 3.

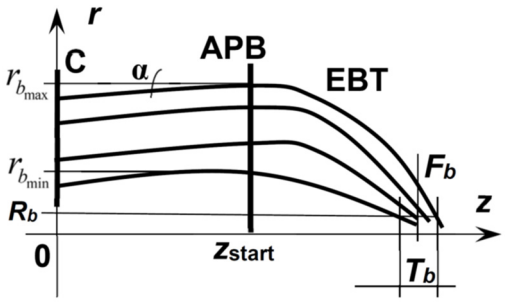

Figure 3. Input and output parameters of simulated hollow EB.
C – cathode surface, APB – anode plasma boundary, EBT – EB trajectories

The main problem in this research is the possibility of changing the radius of the focal beam ring R_b by changing the magnetic lens parameters, which has been described before. Dependencies of EB focus position on acceleration voltage U_{ac}, EB current I_b, and angle of beam divergence α are also necessary from the point of view of the practical application of HVGDEG.

Corresponding analytical relations for describing the approach of simulating the trajectories of the electron beam will be given in the next section of the article. It should be pointed out that the main aim of this research is to calculate the EB trajectories in the region of free movement in the AP in the magnetic field of a short-focusing lens, after acceleration of electrons in the electric field of the cathode fall region. The task of simulating electrode systems in the cathode fall region, including defining AP boundary position, is separate. This task, for the HVGD system with the plane cathode surface, like presented in Fig. 2, has been considered early in the paper [16].

BASIC MATHEMATICAL RELATIONS

It is well-known from the basic conceptions of electron optics that the inductivity of magnetic lenses in electrode systems, similar to those presented in Fig. 2, is interpolated with an accuracy range of 1,5 – 3 % by the Galejs model [39-42]. The corresponding analytical relation for axial magnetic induction B_{z0} is written via lens electrical and geometry parameters as follows [39–42]:

$$B_{z0} = \frac{1.257 \cdot 10^{-4} I_l N_l}{2 S_l} \left(\frac{z_l + \frac{S_l}{2}}{\sqrt{\left(\frac{D_l}{3}\right)^2 + \left(z_l + \frac{S_l}{2}\right)^2}} - \frac{z_l - \frac{S_l}{2}}{\sqrt{\left(\frac{D_l}{3}\right)^2 + \left(z_l - \frac{S_l}{2}\right)^2}} \right), \tag{1}$$

where I_l is the lens current, A, N_l is the number of lens coils, z_l is the width of lens, m, S_l is the width of nonmagnetic lens gap, m, and D_l is the thickness of the region, where winding wire, m. Precision construction of short magnetic lens with defining the geometry parameters z_l, S_l, and D_l is given in paper [16].

With known axial magnetic inductivity distribution $\mathbf{B}_{z0}(\mathbf{z})$, calculated using relation (1), its transversal distribution at every point on the longitudinal coordinate z in the simulated electrode system, corresponding to Galejs model, simply recalculated as expansion to Taylor series for B_r and B_z components as follows [39 – 42]:

$$B_r = -\frac{r}{2}B'_{z0} + \frac{r^3}{16}B'''_{z0} + \ldots; \quad B_z = B_{z0} - \frac{r^2}{4}B''_{z0} + \ldots . \tag{2}$$

For calculation the EB trajectories in the region of free movement in magnetic field of focusing lens, which induction is calculated by relations (1, 2), such important physical effects have been taking into account [39 – 45].

1. Owns space charge of beam electrons.
2. Space charge of ions of residual gas, which compensate the self space charge of beam electrons.
3 Magnetic focusing of an electron beam in an ionized gas, or pinch-effect, as relativistic effect in the condition of space charge of beam electrons compensation. Really, for considered acceleration voltage, smaller than 500 kV, this effect can be ignored [39 – 42]. Results of computer simulation, given in next part of the article, are confirm this presumption.
4. Influence of the magnetic field of focusing lens and twisting of the electrons' trajectories in it.
5. Dissipation of beam electrons on the atoms of residual gas corresponding to Rutherford model [44 – 46].

Therefore, corresponding set of algebraic-differential equation is written as follows [39 – 42]:

$$n_{i0} = \sqrt{\pi} r_b^2 B_i p n_e \sqrt{\frac{M\varepsilon_0 n_e}{m_e U_c}} \exp\left(-\frac{U_c}{\varepsilon_0 n_e r_b^2}\right), \quad f = \frac{n_e}{n_{i0} - n_e}; \quad C = \frac{I_b\left(1 - f - \beta^2\right)}{4\pi\varepsilon_0 \sqrt{\frac{2e}{m_e}} U_c^{3/2}};$$

$$\tan\left(\frac{\theta_{\min}}{2}\right) = \frac{10^{-4} Z_a^{4/3}}{2\gamma\beta^2}; \tan\left(\frac{\theta_{\max}}{2}\right) = \frac{Z_a^{3/2}}{2\gamma\beta^2}; \tag{3}$$

$$\bar{\theta}^2 = \frac{8\pi r_b^2 n Z_a^2 z}{\beta^4\gamma^2} \ln\left(\frac{\theta_{\max}}{\theta_{\min}}\right), \quad \theta = \frac{d^2 r_b}{dz^2} dz + \theta_s, \quad \frac{d^2 r_b}{dz^2} = \frac{C\left(R_{\max} - R_{\min}\right)}{l_{an}} - \frac{e\left(R_{\max} - R_{\min}\right) B_{z0}^2}{16 m_e U_c},$$

where U_c is acceleration voltage, I_b is beam current, p is residual gas pressure, $R_{\max}$ is maximal radius of EB, $R_{\min}$ is its minimal radius, l_{an} is length of anode aperture, B_i is the level of gas ionizing, n_e is concentration of electrons, m_e is mass of electron, ε_0 is dielectric constant, f is level of beam space charge compensation by ions of residual gas, $\theta_{\min}$ is minimal scattering angle, $\theta_{\max}$ is maximal scattering angle, Z_a – charge of nuclear for residual gas atoms, $\beta = v/c$ is relation of electrons velocity v to light velocity c, r_b is EB radius, n is concentration of gas atoms, $\bar{\theta}$ is average angle of electrons dissipation.

Generally, the set of equations (3) is only slightly different from well-known equations for EB with point focus by taking into account maximal and minimal radius of hollow cylindrical EB [48, 49].

Dependence of EB current on acceleration voltage and residual gas pressure $I_b(U_c, p)$ for HVGDEG is usually considered as a simple power function [28, 29]:

$$I_b\left(U_c, p\right) = C_I U_c^m p^k, \tag{4}$$

where C_I, m and k is semiempirical coefficients, which depended on the geometry of electrodes system, operation gas and cathode material [28, 29]. As it is proven in the theory of HVGD, the values of coefficients m and k are always lead in the range from 1 to 2.

In elaborated computer software the set of algebraic-differential equations (3), taking into account (1, 2, 4), has been solved using the fourth-order Runge – Kutta method [47 – 57].

Another approach to finding the trajectories of relativistic EB in the high-frequency electromagnetic fields has been proposed in papers [58 – 60]. This approach is generally based on statistical analysis of experimental results using microcomputers, connected with experimental equipment.

PARTICULARITIES OF SIMUALTION TECHNIQUE

For providing computer simulation of EB trajectories, the original computer software EBTIAE (Electorn Beam Trajectories Interpolation, Approximation and Extrapolation), created directly for analyzing parameters of short-focus

EB, propagated at low pressure in ionized gas, has been used [43]. This software has been developed using the advanced means of Python programing language, particularly, paradigms of functional and matrix programming [32 – 34].

It should be pointed out that the main particularity of elaborated computer software is its multifunctionality and orientation to solving different practical tasks connected with simulation of EB propagation in ionized gas [32 – 34]. Another distinguishing feature of elaborated software is the inclusion of advanced means of graphic user interface for each scientific and engineering task, which is solved. Therefore, for the convenience of users working with the developed software, all the various tasks, which can be solved, are located on separate tabs of the corresponding graphic window [32 – 34]. For example, one of these windows is a window in which an important engineering problem of simulating the guiding of short-focus EB in the equipotential channel in the field of short magnetic lenses is solved. The corresponding interface window of elaborated computer software is presented in Fig. 4.

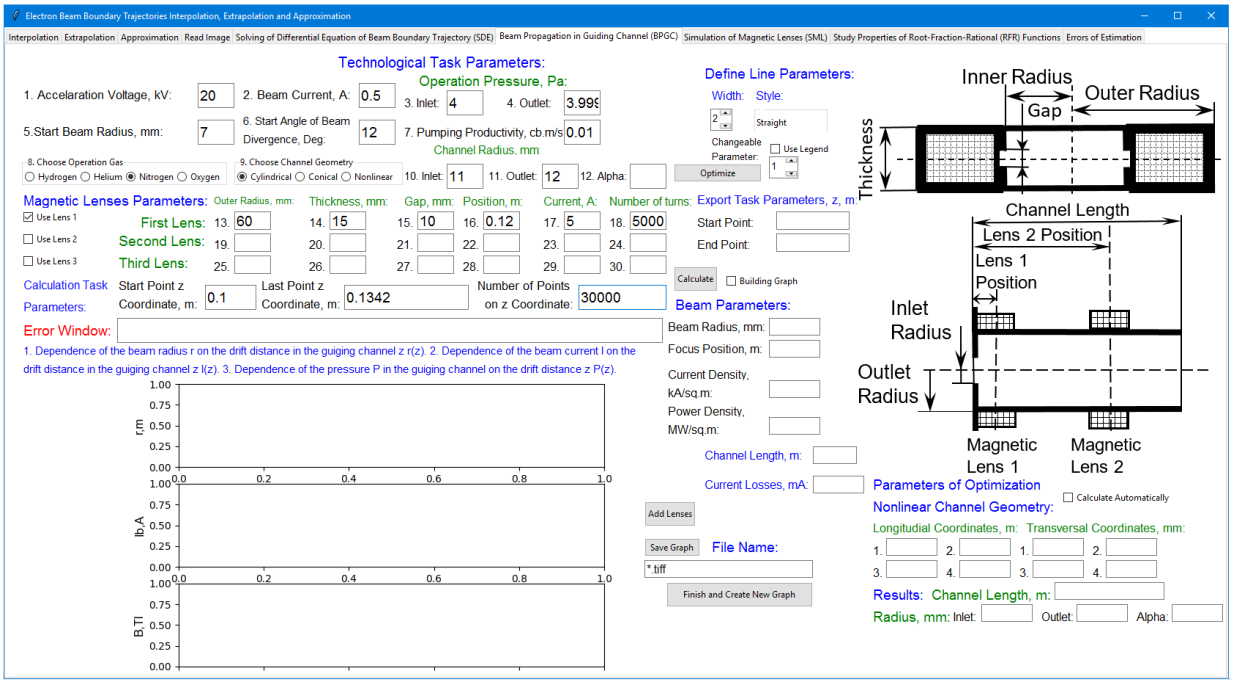

Figure 4. Interface window of the elaborated computer software EBTIAE, designed for solving the task of short-focus EB propagation in the equipotential channel in the field of magnetic lens. Screen copy

But it should be pointed out that solving the problem of finding the trajectories of hollow EB, propagated in an electrode system with a plane cathode, a cylindrical anode, and one focusing magnetic lens, is generally different and needs a specific approach for defining simulation parameters. Main presumptions in this aspect are connected with basic conceptions of vacuum science and technology [61, 62] and can be formulated as follows.

1. Inlet and outlet operation pressures are given as close values, which correspond to operation pressure in the electron gun, but outlet pressure has to be slightly smaller. For example: inlet pressure – 4 Pa, and outlet – 3.999 Pa.

2. Pumping productivity is taken as an extra small value, for example, 0.001 m³/s.

3. Inlet and outlet channel radii are given as close values, which correspond to the maximum value of the EB radius $r_{b_{\max}}$, but they are slightly greater. For example: if $r_{b_{\max}} = 10$ mm, the inlet channel radius can be taken as 11 mm, and the outlet, correspondingly, as 12 mm.

It is obvious that with such limitations and assumptions on the parameters of the computer model, the description of the propagation of a hollow EB in an electrode system with a plane cathode, a cylindrical anode, and a focusing magnetic lens is completely correct. For the real tasks, the parameters of the virtual channel for EB propagation are selected so that its length corresponds to the extent of the electrons' drift region along the longitudinal coordinate z, up to the ring focus of the EB. Thus, the set simulation problem is completely reduced to the previously solved problem of simulating the process of guiding an EB with a point focus in an equipotential channel. In general, such an approach simplifies the structure of the developed computer software and its operation. It is generally clear that the expansion of the range of engineering problems solved in one software complex always leads to significant complications in computer software.

OBTINED SIMULATION RESULTS

Let's considering now some simulation tasks, which given basic dependences of position F_b and radius R_b of focal beam ring on location of lens z_l, lens current I_l and number of coils N_l, as well as acceleration voltage U_c and EB current I_b.

Task 1. Calculate EB trajectories for parameters of the beam and electromagnetic lens, given in Table 1.

Obtained graphic dependences for different values of start EB radius r_{b0} are given in Fig. 5.

Table 1. Parameters of EB and electromagnetic lens for Task 1

Type of parameters	#	Parameter	Value
EB propagation parameters	1.	Acceleration voltage, kV	20
	2.	Beam current, A	0.5
	3.	Operation pressure, Pa	4
	4.	Type of gas	N_2
	5.	Pumping productivity, m^3/s	$1.7 \cdot 10^{-3}$
	6.	Start point on *z* coordinate, m	0.1
	7.	Maximal value of EB radius, mm	10
	8.	Minimal value of EB radius, mm	7
	9.	Angle of EB divergence, degree	12
Parameters of magnetic lens	1.	External radius, mm	60
	2.	Thickness, mm	15
	3.	Gap, mm	10
	4.	Position, m	0.12
	5.	Current, A	5
	6.	Number of turns	5000

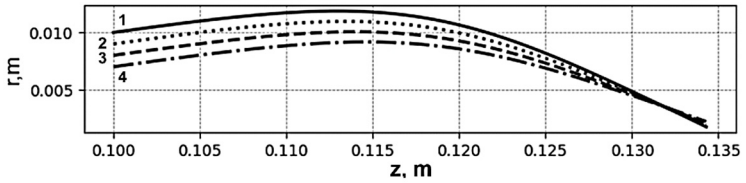

Figure 5. Simulation results, have been obtained for Task 1.
1 – r_{b0} = 10 mm; 2 – r_{b0} = 9 mm; 3 – r_{b0} = 8 mm; 4 – r_{b0} = 7 mm

As it is clear from the obtained simulation results, electron beam trajectories, started from different points by the transversal coordinate r, are focused by a short magnetic lens in one point with the position of the focal beam ring F_b = 0.1323 m and the radius of the focal ring R_b = 4.63 mm. The thickness of the focal ring for this task is T_b = 2.4 mm. Generally, simulation results, obtained by solving this task, confirm the basic statement of electron optics, that all electrons, which started from different points at the same angle, when they have the same velocity, are collected by the magnetic lens to the single-point region, located at the corresponding distance [38 – 42].

Task 2. Calculate EB trajectories for parameters, given in Table 1, but for angle of EB divergence $\alpha = 8^0$ and minimal value of EB radius $r_{b_{\min}} = 5$ mm. Compare obtained results with results, which have been obtained in the Task 1.

The graphic dependencies, have been obtained by solving this task for EB trajectories with different start radii r_{b0}, are given in Fig. 6.

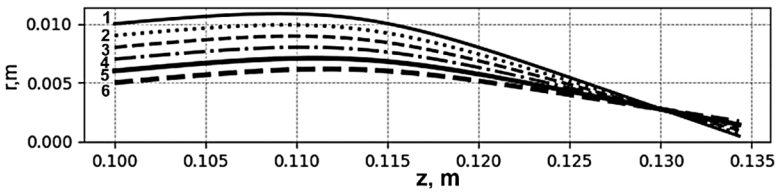

Figure 6. Simulation results, have been obtained for Task 2.
1 – r_{b0} = 10 mm; 2 – r_{b0} = 9 mm; 3 – r_{b0} = 8 mm; 4 – r_{b0} = 7 mm; 5 – r_{b0} = 6 mm; 6 – r_{b0} = 5 mm

It is obvious, that for this simulation task EB trajectories also converge at the region of one point with focal parameters F_b = 0.1295 and R_b = 2.61 mm. The thickness of the focal beam ring in this case is T_b = 1.8 mm. Generally, for a smaller value of EB divergence angle α, the position of focus approaches the cathode, and the radius of the focal ring and its thickness become smaller. These results are also in good agreement with the basic principles of electron optics [38 – 42].

Task 3. Calculate EB trajectories for parameters given in Table 1, but for different angles of EB divergence: $\alpha = 12^0$, $\alpha = 10^0$, $\alpha = 8^0$, and $\alpha = 6^0$. Compare the obtained results with the results, which just have been obtained in the Task 1 and Task 2.

The graphic dependencies, have been obtained by solving this task for different angles of EB divergence α and start radius r_{b0} are given in Fig. 7.

From the computer-solved of this simulation task, it is clear that with the dispersion of angles of EB divergence, the position of the focal ring is changed, and its thickness becomes generally greater. Position of focal ring without divergence of angles corresponds to Task 1, F_b = 0.1323 m, but since from the start point with radial coordinate r_{b0} = 10 mm inlet

few EB trajectories with different divergence angles, which are smaller, that the basic angle $\alpha = 12^0$, the focal beam ring approaches to the cathode slightly. For this task, the corresponding value is $F_b = 0.1284$ m. The thickness of the focal ring is also becoming significantly greater, $T_b = 4.4$ mm. Therefore, with the dissipation of divergence angles of electrons, the focal power density of EB is significantly smaller. Generally, this result also fully corresponded to basic principles of electron optics and had to be taken into account in the construction of electron guns for industrial applications [38, 42].

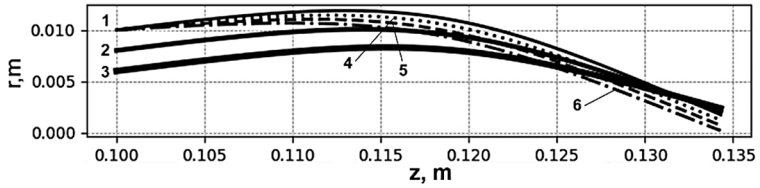

Figure 7. Simulation results, have been obtained for Task 3.
1 – $r_{b0} = 10$ mm, $\alpha = 12^0$; 2 – $r_{b0} = 8$ mm, $\alpha = 12^0$; 3 – $r_{b0} = 6$ mm, $\alpha = 12^0$; 4 – $r_{b0} = 10$ mm, $\alpha = 10^0$; 5 – $r_{b0} = 10$ mm, $\alpha = 8^0$; 6 – $r_{b0} = 5$ mm, $\alpha = 8^0$

Task 4. Calculate EB trajectories for parameters given in Table 1, but for the position of the magnetic lens, $z_l = 0.13$ mm and the minimal value of EB radius $r_{b_{\min}} = 5$ mm. Provide a simulation also for another gap of the magnetic lens, $G_l = 5$ mm. Compare the obtained results with the results, which have been obtained in Task 1.

The graphic dependences, have been obtained by solving this task are given in Fig. 8.

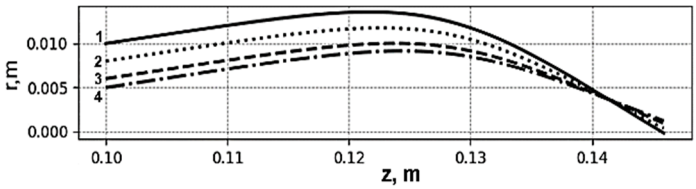

Figure 8. Simulation results, have been obtained for Task 4.
1 – $r_{b0} = 10$ mm; 2 – $r_{b0} = 8$ mm; 3 – $r_{b0} = 6$ mm; 4 – $r_{b0} = 5$ mm

As shown in Fig. 8, when the magnetic lens is moved further away from the cathode, the ring focus of the electron beam also shifts to a greater distance. In this case, $F_b = 0.1418$ m. On the contrary, the radius of the focal ring is generally similar: $R_b = 4.65$ mm and $T_b = 2.53$ mm. It is also interesting that for $G_l = 5$ mm the simulation results are similar, with no significant difference from those that are given in Fig. 8.

Task 5. Calculate EB trajectories for the same EB and lens parameters, as in Task 4, but for different currents of the magnetic lens: $I_l = 4$ A and $I_l = 6$ A.

The graphic dependencies, have been obtained by solving this task, are given in Fig. 9.

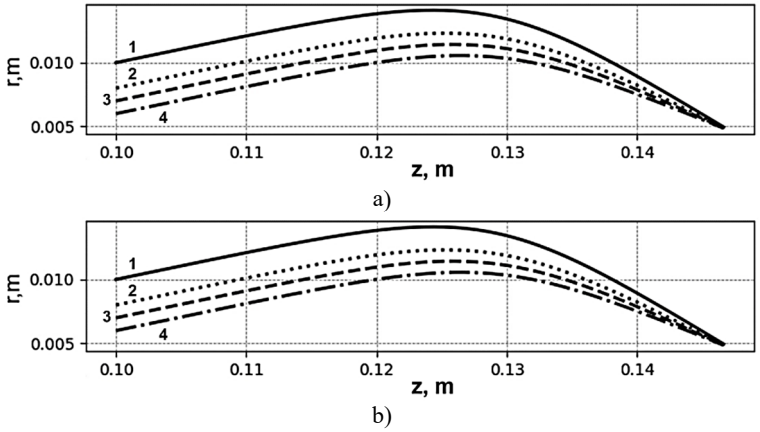

Figure 9. Simulation results, have been obtained for Task 5.
a – $I_l = 4$ A, b – $I_l = 6$ A. 1 – $r_{b0} = 10$ mm; 2 – $r_{b0} = 8$ mm; 3 – $r_{b0} = 6$ mm; 4 – $r_{b0} = 5$ mm

It is clear from the obtained dependencies that in the case of reducing the current of the magnetic lens, the ring focus of the hollow conical EB is located further from the cathode. If in Task 4, in the case of $I_l = 5$ A, the value of $F_b = 0.1418$ m, for $I_l = 4$ A, this value is greater, $F_b = 0.1482$ m. And in this case, the radius of the focal beam ring is also greater, the corresponding value is $R_b = 5.1$ mm. On the contrary, as it is clear from Fig. 9, b, in the case of increasing the current of the magnetic lens, the ring focus of EB approaches the cathode, and the radius of the focal ring becomes smaller. For example, in case $I_l = 4$ A corresponding EB parameters are $F_b = 0.138$ m and $R_b = 2.4$ mm. Therefore, changing of

magnetic lens current is a very suitable way to adjust the parameters of forming EB to the requirements of the technological process, for example, to the wire diameter in technologies of three-dimensional printing by metal [1 – 16].

Task 6. Calculate EB trajectories for the same EB and lens parameters, as in Task 1, but for different number of turns in magnetic lens: $N_l = 4000$ and $N_l = 6000$.

The graphic dependences, have been obtained by solving this task are given in Fig. 10.

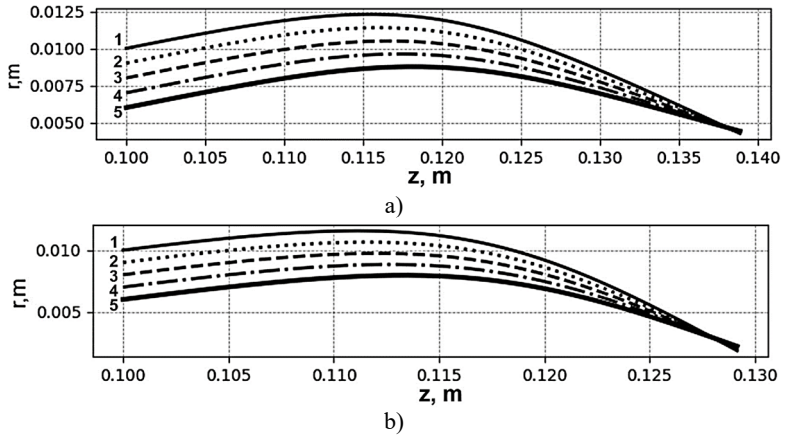

Figure 10. Simulation results, have been obtained for Task 6.
a – $N_l = 4000$, b – $N_l = 6000$. 1 – $r_{b0} = 10$ mm; 2 – $r_{b0} = 9$ mm; 3 – $r_{b0} = 8$ mm; 4 – $r_{b0} = 7$ mm; 5 – $r_{b0} = 7$ mm

It is clear from the obtained dependencies, presented in Fig. 5 and Fig. 10, that in the case of reducing the number of turns of the magnetic lens, the ring focus of the hollow conical EB is also located further from the cathode, and the radius of the focal beam ring becomes greater. On the contrary, in the case of increasing the number of turns, the ring focus was located nearer to the cathode, and the radius of the focal beam ring became smaller. But the thickness of the focal ring with changing the number of turns of the magnetic lens is generally similar. Corresponding values for this example have been obtained as results of a computer simulation, are presented in Table 2.

Table 2. Focal parameters of EB for simulation Task 6

N_l	F_b, m	R_b, mm	T_b, mm
4000	0.1375	5.0	2.44
5000	0.1323	4.63	2.4
6000	0.1283	2.5	2.42

It should also be pointed out that increasing the number of turns in the magnetic lens gives the same influence to the focus position and focal beam ring as increasing the lens current. This fact is simply explained by relation (1), because the product of the quantities $I_l N_l$ appears directly in the numerator of this formula. Really, this rule is very important from a practical point of view and will be considered carefully in the next section of the article.

Task 7. Calculate EB trajectories for the simulation task parameters, given in Table 1, but for different values of acceleration voltage: $U_c = 15$ kV and $U_c = 25$ kV.

The graphic dependencies, have been obtained by solving this task, are given in Fig. 11.

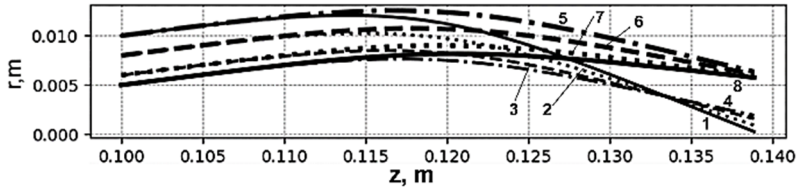

Figure 11. Simulation results, have been obtained for Task 7.
1 – $r_{b0} = 10$ mm, $U_c = 15$ kV; 2 – $r_{b0} = 8$ mm, $U_c = 15$ kV; 3 – $r_{b0} = 6$ mm, $U_c = 15$ kV; 4 – $r_{b0} = 5$ mm, $U_c = 15$ kV; 5 – $r_{b0} = 10$ mm, $U_c = 25$ kV; 6 – $r_{b0} = 8$ mm, $U_c = 25$ kV; 7 – $r_{b0} = 6$ mm, $U_c = 25$ kV; 8 – $r_{b0} = 5$ mm, $U_c = 25$ kV

It is clear from the obtained simulation results that with increasing acceleration voltage, the focal beam ring is located further from the cathode and its radius becomes greater. Values of these EB parameters, obtained as a result of solving this simulation task, are presented in Table 3.

Table 3. Focal parameters of EB for simulation Task 7

U_c, kV	F_b, m	R_b, mm	T_b, mm
15	0.1311	3.95	2.8
20	0.1323	4.63	2.4
25	0.1398	5.21	1.9

Task 8. Calculate EB trajectories for the simulation task parameters, given in Table 1, but for different values of EB current: I_b = 0.3 A and I_b = 0.7 A.

The graphic dependencies, have been obtained by solving this task are given in Fig. 12.

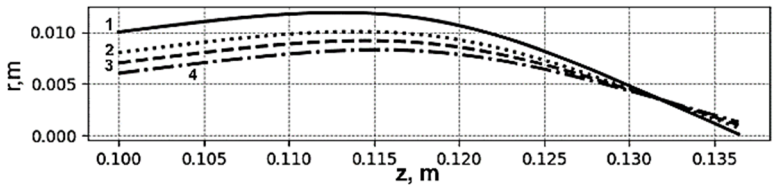

Figure 12. Simulation results, have been obtained for Task 8.
1 – r_{b0} = 10 mm; 2 – r_{b0} = 8 mm; 3 – r_{b0} = 7 mm; 4 – r_{b0} = 6 mm

It is generally clear that dependencies for EB trajectories, presented in Fig. 12 and obtained for the case I_b = 0.3 A, are in particularity the same as dependencies for the case I_b = 0.5 A, given in Fig. 5. Therefore, focal parameters of EB are also the same. For the value of EB current I_b = 0.7 A, the graphs of EB trajectories also do not practically differ from the graphs already presented in Fig. 5 and Fig. 12. Therefore, EB focal parameters generally don't depend on the current of EB. From the theoretical point of view, this fact can be simply explained by the compensation of the owner space charge of electrons by the positive ions of ionized gas [39 – 42].

The same simulation results have been obtained with changing operation pressure from 4 Pa to 7 Pa, generally, EB trajectories aren't deferred, and focal parameters were the same as in Task 1.

Experimental focal parameters of hollow EB, have been obtained with the values of its input parameters and parameters of magnetic lens, given in Table 1, but for different acceleration voltage and number of turns of magnetic lens, are presented in Table 4.

Table 4. Measurement focal parameters of hollow EB for different acceleration voltage

U_c, kV	N_l	F_b, m	R_b, mm	T_b, mm
15	5000	0.129	3.42	2.67
20	4000	0.1384	4.83	2.12
20	5000	0.1337	4.48	2.08
20	6000	0.1256	2.37	2.31
25	5000	0.1419	5.18	1.57

Overall, it is clear that the obtained simulation results presented in Tables 2 and 3 and the experimental data on the focal EP parameters presented in Table 4 are in excellent agreement. The difference between them does not exceed 15%. Therefore, the developed software can be effectively used by design engineers for preliminary evaluation of the focal parameters of a hollow EP focused by a magnetic lens. Corresponding practical recommendations will be given in the next subsection of the article.

ANALIZING OF OBATINED SIMULATION RESULTS AND PRACTICAL RECOMMENDATIONS

Generally, the provided scientific studies have shown that the developed computer software, based on the mathematical approach and physical assumptions described in the previous subsections, yields accurate calculations of the hollow EP focal parameters, which correlate well with the obtained experimental data. Therefore, it is strongly recommended to use this software in the simulation and computer-aided design of an improved HVGDEG for future industrial applications.

On the basis of the provided simulation and obtained theoretical results, some important practical recommendations in the aspect of designing novel HVGDEG constructions with the plane cathode and magnetic EB focusing have been formulated. Generally, the most significant physical effects that characterize dependencies between input and output EB parameters are as follows. Generally, the provided scientific studies have shown that the developed computer software, based on the mathematical approach and physical assumptions described in the previous subsections, yields accurate calculations of the hollow EP focal parameters, which correlate well with the obtained experimental data. Therefore, it is strongly recommended to use this software in the simulation and computer-aided design of an improved HVGDEG for future industrial applications.

1. In accordance with the law of electron optics, beam electrons that have the same speed and initial divergence angles, but start in the region of free motion with different transverse coordinates r_{b0}, are focused after passing through a short magnetic lens at one point.

2. As the divergence angle of the electron beam increases, its ring focus moves further from the cathode surface, and the radius of the focal ring in this case becomes greater.

3. With a large spread of the initial angles of entry of the beam electrons into the drift region in the magnetic lens, the thickness of the focal ring increases significantly, which leads to a significant decrease in the electron beam current density on the workpiece. In general, at small entry angles, the focus of the electron beam is located closer to the cathode surface, and at large entry angles, it is further away. On the one hand, a large spread of the entry angles of the beam

electrons at the entrance to the drift region in the AP, caused by their collisions with residual gas atoms, is a characteristic feature of the operation of HBGD electron sources. Therefore, electrons with different entry angles are scattered after passing through the magnetic lens. However, if the electron beam current density at the focus of the ring is sufficient to perform a specific technological operation, magnetic focusing offers significant advantages in terms of the ability to control the focal parameters of the beam, including the focus position, the radius of the focal ring, and its thickness. The corresponding theoretical foundations for estimating the thickness of the focal ring EB are considered in [16].

4. When the magnetic lens is moved to a greater distance from the cathode, the ring focus of the electron beam is also located further away. The thickness of the focal ring in this case is generally similar.

5. In the case of reducing the current of the magnetic lens, the ring focus of the hollow conical EB is located further from the cathode, and its radius becomes greater. On the contrary, in the case of increasing current of the magnetic lens ring, the focus of EB is approached to the cathode, and the radius of the focal ring becomes smaller. But the thickness of the focal ring in this case is also generally similar.

6. Generally, increasing the number of turns in the magnetic lens gives the same influence on the focus position and the radius of the focal beam ring as increasing the lens current.

7. In the case of reducing the number of turns of the magnetic lens, the ring focus of the hollow conical EB is located further from the cathode, and its radius becomes greater. On the contrary, in the case of an increasing number of turns of the magnetic lens, the ring focus of EB approaches the cathode, and the radius of the focal ring becomes smaller. The thickness of the focal ring in this case is generally similar.

8. In case of changing the magnetic lens gap, the focus position and focal ring radius are generally unchanged.

9. In the case of increasing acceleration voltage, the ring focus of the EB is located further away from the cathode, and the radius of the focal ring becomes larger. Among the dependencies that have been obtained and studied, this is the most clearly expressed. When the accelerating voltage changes by 5%, the position of the beam focus and its focal diameter always change within 15 - 20%. Therefore, the correct selection and stabilization of the accelerating voltage using the appropriate design tools for high-voltage technology is a primary necessary condition for the stable operation of electron-beam technological equipment with magnetic focusing of the EP [16]. In general, this fact is quite simply explained by the basic laws of electron optics, since, as is known, the focusing power of a magnetic lens is very strongly dependent on the velocity of electrons, which is directly related, namely, to the accelerating voltage [39 – 42].

10. When the EB current and the HVGD operating pressure change, the focal position and focal ring radius generally remain unchanged. This effect is explained primarily by the fact that the beam electrons move under conditions of space charge compensation by residual gas ions. Generally, the EB current and the operating pressure under VTR ignition conditions are related by relation (4).

Consequently, in accordance with the rules of physical laws, which are described above, general recommendations regarding the engineering development of the EB equipment with HVGDEG, which uses a short magnetic focusing lens for forming EB, have been formulated as follows.

1. The basic condition of updating HVGDEG with magnetic focusing to meet certain requirements of the technological process is defining the correct acceleration voltage. The values of beam current and operation pressure are defined after that by the necessary current density for melting the moving wire. Corresponding analytical relations are given in the paper [29].

2. Changing the position of the magnetic lens relative to the cathode allows, when designing electron-beam equipment, positioning the focus of the electron beam at a given distance in the chamber of the item treatment in accordance with the requirements of the technological process.

3. The correct choice of the EB focus position and the radius of its focal ring can be done in two ways: by changing the current of the focusing magnetic lens or by changing the number of its turns. When designing an electron beam installation, the best method is to increase the number of lens turns rather than to increase its current, since in this case the lens heats up less and its heating has less effect on the parameters of the technological process. On the other hand, the method of changing the lens current is easier to implement and can be implemented when reconfiguring technological equipment for another type of product, as well as directly during the realization of the technological process.

4. The installation can be easily reconfigured to heat a wire of a different diameter by changing the magnetic lens current, which allows the use of HVGDEG with magnetic focusing of the EB in small-scale production while maintaining the high quality of the products obtained. This technology is extremely cheap and very effective, since it does not require highly qualified service personnel to disassemble the electron gun to reconfigure the equipment for a new technological operation.

5. Automatic control of the focus position of the EB during the technological process can be easily accomplished by changing the current of the magnetic lens on the small values.

In general, the obtained simulation results showed that the flat-cathode HVGDEG with magnetic focusing of the EB, as a technological tool, has a number of advantages over guns with a spherical cathode and electrostatic focusing in the technologies of three-dimensional printing by metal. They, like guns with electrostatic focusing, form a hollow converging EB with a ring focus and provide uniform heating of the wire along the perimeter, but are much easier to operate. In addition, an important technological advantage of guns with magnetic focusing of the EB is the ability to adjust the radius of the focal ring by changing the current of the magnetic lens. In general, the theoretical studies have

shown that this type of HVGDEG can be successfully used for melting wires or rods with various diameters, from 0.5 to 10 mm. Further development and application of such advanced technologies is very promising for the development of the transport industry and mechanical engineering and the chemical, aviation, and space industries, in particular, for the production and reconstruction of blades of aircraft and marine engines.

CONCLUSIONS

Provided numerical computer experiments and scientific research directed to the study of focusing EB trajectories with different parameters in short magnetic lenses, showing that in the physical conditions of HVGD, it is possible to form a hollow EB with ring focus. Therefore, uniform heating of treated wire or rods is guaranteed. Since, in comparison with experimental results, the accuracy of the simulation is very high, in the range of 5 – 15%, the elaborated computer software with corresponding assumptions for creating the simulation tasks can be successfully used on the preliminary steps of HVGDEG engineering designing for certain industrial technologies' three-dimensional printing by metal.

Based on the obtained theoretical and experimental results, important physical laws and rules have also been formulated, which can be further effectively used for the design of electron-beam technological equipment using the developed software.

Generally, the provided research has shown that by using HVGDEG with a plane cathode and a short magnetic lens, the formation of hollow EB with a radius of the focal ring range of 1 – 5 mm. Using EB with such parameters for melting wire or rods with a diameter from 0.5 to 10 mm is really possible.

A significant technological advantage of using magnetic focusing for electronic lasers is the ability to easily change the focus position and focal ring radius by adjusting the magnetic lens current. This allows for easy reconfiguration of the process equipment for new product types, as well as automatic control of the focus position during the process. The developed software can also be effectively used to select the optimal magnetic lens current.

In general, the conducted studies have shown that the development and wide implementation in industry of the HVGDEG with a flat cathode and magnetic focusing of the electron beam will significantly contribute to the further development and improvement of modern electron-beam technologies of three-dimensional printing on metal. Today, the engineers and experts working in the fields of production of transport vehicles, mechanical engineering, chemical industry, shipbuilding, aircraft construction, and space industry are most interested in the use and further improvement and development of such advanced technologies.

Overall, the conducted research has shown that the development and widespread industrial adoption of a flat-cathode HTEG with magnetic focusing of the electron beam will significantly contribute to the further development and improvement of modern electron-beam 3D printing technologies on metal. Currently, engineers and specialists working in the vehicle manufacturing, mechanical engineering, chemical industry, shipbuilding, aircraft manufacturing, and space industries are showing the greatest interest in the use and further improvement of such promising technologies.

Acknowledgements

The work has been carried out at the Scientific and Educational Laboratory of Electron Beam Technological Devices of the National Technical University of Ukraine “Igor Sikorsky Kyiv Polytechnical Institute”. It has been financially supported by the Ministry of Education and Science of Ukraine. Priority area: new substances and materials; priority thematic area: ceramic and composite materials and coatings for extreme conditions of use; state registration number is 0124U001525. The experimental research, which has been provided, is supported by the Joint Stock Company, Scientific and Industrial Association “Chervona Hvylia”.

ORCID

Igor V. Melnyk, https://orcid.org/0000-0003-0220-0615; **Serhii B. Tuhai**, https://orcid.org/0000-0001-7646-1979
Mykhailo Yu. Skrypka, https://orcid.org/0009-0006-7142-5569; **Dmytro V. Kovalchuk,** https://orcid.org/0000-0001-9016-097X

REFERENCES

[1] Wohlers Report 2023. Analysis. Trends. Forecasts. 3D Printing and Additive Manufacturing State of the Industry. ASTM International. (2023). https://wohlersassociates.com/product/wr2023/
[2] An Additive Manufacturing Breakthrough: A How-to Guide for Scaling and Overcoming Key Challenges. White Paper. World Economic Forum, edited by F. Betti, C. Seidel, M. Meboldt, (2022). https://www3.weforum.org/docs/WEF_Additive_Manufacturing_Breakthrough_2022.pdf
[3] *A Guide to Additive Manufacturing*, edited by D. Godec, J. Gonzalez-Gutierrez, A. Nordin, E. Pei, and J.U. Alcazar, (Springer, 2022). https://doi.org/10.1007/978-3-031-05863-9
[4] M. Armstrong, H. Mehrabi, N. Naveed, Journal of Manufacturing Processes, **84**, 1001 (2022). https://doi.org/10.1016/j.jmapro.2022.10.060
[5] Identifying current and future application areas, existing industrial value chains and missing competences in the EU, in the area of additive manufacturing (3D-printing). European Commission. Final Report. Brussels, 15th of July, 2016. https://op.europa.eu/en/publication-detail/-/publication/b85f5e09-7e2b-11e6-b076-01aa75ed71a1/language-en
[6] W. Frazier, Journal of Materials Engineering and Performance, **23**(6), (2014). https://doi.org/10.1007/s11665-014-0958-z
[7] *Additive Manufacturing for the Aerospace Industry*, edited by: F. Froes, and R. Boyer, (Elsevier, 2019). https://doi.org/10.1016/C2017-0-00712-7
[8] R. Brooke, https://www.tctmagazine.com/additive-manufacturing-3d-printing-news/additive-manufacturing-can-lower-aircraft-building-and-oper/

[9] TCT Team, https://www.tctmagazine.com/additive-manufacturing-3d-printing-news/sciaky-metal-3d-printing-lockheed-martin-space/
[10] K. Taminger, and R. Hafley, "Electron beam freeform fabrication: A rapid metal deposition process," *Proceedings of the 3rd Annual Automotive Composites Conference*, (Troy, MI, USA, September, 9–10, 2003.
[11] S. Stecker, K.W. Lachenberg, H. Wang and R.C. Salo, in: *Proceedings of FABTECH and AWS Welding Show*, (Atlanta, GA, USA, 2006). pp. 35–46.
[12] Patent #8,344,281 B2, 2013. (USA).
[13] F. Pixner, F. Warchomicka, P. Patrick, A. Steuwer, H. Colliander, R. Pederson, and N. Enzinger, Materials, **13,** 3310 (2020). https://doi.org/10.3390/ma13153310
[14] W.J. Sames, F.A. List, S. Pannala, R.R. Dehoff, and S.S. Babu, International Materials Reviews. **61**, 5 (2016). https://doi.org/10.1080/09506608.2015.1116649
[15] I. Melnyk, S. Tuhai, O. Kovalenko, M. Skrypka, and D. Kovalchuk, in: *2024 IEEE 7th International Conference on Smart Technologies in Power Engineering and Electronics (STEE),* (Kyiv, Ukraine, 2024), pp. TT3.01.1-TT3.01.6. https://doi.org/10.1109/STEE63556.2024.10748050
[16] I.V. Melnyk, S.B. Tugay, V.O. Kyryk, and I.S. Shved, System Research and Information Technologies, **2021**(3), 17 (2021). https://doi.org/10.20535/SRIT.2308-8893.2021.3.02 (in Ukrainian)
[17] H. Xu, X. Sang, B. Yang, Y. Peng, and J. Fan, Chinese journal of vacuum science and technology, **41**(3), 284 (2021). http://cjvst.cvs.org.cn/en/article/doi/10.13922/j.cnki.cjvst.202005028?viewType=citedby-info
[18] Chang Jiawei, Li Shengbo, Lin Zhishu, Bai Fengmin, Li Guozheng, and Bai Zongzheng, Chinese journal of vacuum science and technology, **44**(5), (2024). http://cjvst.cvs.org.cn/en/article/doi/10.13922/j.cnki.cjvst.202401009
[19] Gu Liang, Yang Jie, Zhao Hua, Tan Wei, and Li Jinrong, Chinese journal of vacuum science and technology, **44**(2), 184 (2024). http://cjvst.cvs.org.cn/en/article/doi/10.13922/j.cnki.cjvst.202306003
[20] Qui Yufan, Li Shengbo, Zheng Xinjian, Fu Shengping, and Bai Fengmin, Chinese journal of vacuum science and technology, **41**(11), 1094 (2021). http://cjvst.cvs.org.cn/en/article/doi/10.13922/j.cnki.cjvst.202101027
[21] Deng Chenhui, Wang Yan, Liu Junbiao, and Han Li, Chinese journal of vacuum science and technology, **40**(9), 847 (2020). http://cjvst.cvs.org.cn/en/article/doi/10.13922/j.cnki.cjovst.2020.09.09
[22] Wang Jian, Chinese journal of vacuum science and technology, **40**(4), 381 (2020). http://cjvst.cvs.org.cn/en/article/doi/10.13922/j.cnki.cjovst.2020.04.17
[23] Xiang Yidong, Zhao Ding, Xue Qianzhong, and Li Xiaofei, Chinese journal of vacuum science and technology, **40**(3), 226 (2020). http://cjvst.cvs.org.cn/en/article/doi/10.13922/j.cnki.cjovst.2020.03.08
[24] Wang Yan, Zhao Weixia, Deng Chenhui, Liu Junbiao, and Han Li, Chinese journal of vacuum science and technology, **40**(1), 1 (2020). http://cjvst.cvs.org.cn/en/article/doi/10.13922/j.cnki.cjovst.2020.01.01
[25] Gu Yunting, Lin Yanjian, Yan Baojun, Liu Shulin, Yang Yuzhen, Yu Yang, Wen Kaile, and Wang Yuman, Chinese journal of vacuum science and technology, **39**(12), 1009 (2019). http://cjvst.cvs.org.cn/en/article/doi/10.13922/j.cnki.cjovst.2019.12.11
[26] Huo Weijie, Hu Jing, Cao Xiaotong, Fu Yulei, and Zhao Wansheng, Chinese Journal of Vacuum Science and Technology, **39**(8), 631 (2019). http://cjvst.cvs.org.cn/en/article/doi/10.13922/j.cnki.cjovst.2019.08.03
[27] Fu Xuecheng, Wang Ying, Quan Xueling, Ju Minni, and Wang Fengdan, Chinese journal of vacuum science and technology, **39**(5), 396 (2019). http://cjvst.cvs.org.cn/en/article/doi/10.13922/j.cnki.cjovst.2019.05.07
[28] S.V. Denbnovetsky, I.V. Melnyk, V.G. Melnyk, B.A. Tugai, and S.B. Tuhai, in: *2016 International Conference Radio Electronics & Info Communications UkrMiCo*, (Kyiv, Ukraine, 2016). pp. 1–4. https://ieeexplore.ieee.org/document/7739615
[29] S.V. Denbnovetsky, I.V. Melnyk, V.G. Melnyk, B.A. Tugai, and S.B. Tuhai, in: *2017 IEEE 37th International Conference on Electronics and Nanotechnology ELNANO*, (Kyiv, Ukraine, 2017). pp. 369-373. https://ieeexplore.ieee.org/document/7939781
[30] S.V. Denbnovetsky, V.I. Melnik, I.V. Melnik, and B.A. Tugay, in: *XVIII-th IEEE International Symposium on Discharges and Electrical Insulation in Vacuum*, (ISDEIV, 1998, Eindhoven, The Netherland), vol. 2. pp. 637–640. https://ieeexplore.ieee.org/stamp/stamp.jsp?tp=&arnumber=738530
[31] I.V. Melnik, and S.B. Tugay, Radioelectronics and Communications Systems, **55**(11), (2012). https://doi.org/10.3103/S0735272712110064
[32] I. Melnyk, S. Tuhai, M. Skrypka, T. Khyzhniak, and A. Pochynok, in: *Information and Communication Technologies and Sustainable Development. ICT&SD 2022. Lecture Notes in Networks and Systems*, edited by S. Dovgyi, O. Trofymchuk, V. Ustimenko, and L. Globa, vol. 809, (Springer, 2023). pp. 395–427. https://doi.org/10.1007/978-3-031-46880-3_24
[33] I. Melnyk, A. Pochynok, and M. Skrypka, System Research and Information Technologies, **2024, #4**. (2024). https://doi.org/10.20535/SRIT.2308-8893.2024.4.11 http://journal.iasa.kpi.ua/issue/view/18934/11880
[34] I. Melnyk, A. Pochynok, M. Skrypka, System Research and Information Technologies, **2024**(3), (2024). https://doi.org/10.20535/SRIT.2308-8893.2024.3.05
[35] W. McKinney, *Python for Data Analysis: Data Wrangling with Pandas, NumPy, and Jupyter*, 3rd Edition, (O'Reilly Media, 2023).
[36] F. Chollet, *Deep Learning with Python. Second Edition*. (Manning, 2022).
[37] M. Lutz, *Learning Python*, Fifth Edition. (O'Reilly, 2013).
[38] S. Schiller, U. Heisig, and S. Panzer, *Electron Beam Technology*, (New-York, John Wiley & Sons, 1995).
[39] M. Szilagyi, *Electron and Ion Optics*, (Springer Science & Business Media, 2012).
[40] E. Kasper, and P. Hawkes. *Principles of Electron Optics: Applied Geometrical Optics*. (Elsevier Science, 1989).
[41] P. Grivet, P.W. Hawkes, and A. Septie, *Electron Optics*, (Elsevier, 2013).
[42] *Electron Beams, Lenses, and Optics*, edited by A. B. El-Kareh, (Academic Press, 2012).
[43] B.M. Smirnov, *Theory of Gas Discharge Plasma*, (Springer, 2015).
[44] M.A. Lieberman, and A.J. Lichtenberg. *Principles of Plasma Discharges for Materials Processing*, (New York, Wiley Interscience, 1994).
[45] Yu.P. Raizer, *Gas Discharge Physics*, (New York: Springer, 1991).

[46] J.F. Epperson, *An Introduction to Numerical Methods and Analysis*, Revised Edition, (Wiley-Interscience, 2007).
[47] M.K. Jain, S.R.K. Iengar, and R.K. Jain, *Numerical Methods for Scientific & Engineering Computation*. (New Age International Pvt. Ltd., 2010).
[48] S.C. Chapra, and R.P. Canale, *Numerical Methods for Engineers*, 7th Edition, (McGraw Hill, 2014).
[49] R.L. Burden, J.D. Faires, and A.M. Burden, *Numerical Analysis*, **(**Cengage Learning, 2015).
[50] T. Sauer, *Numerical Analysis*, (Pearson, 2017).
[51] R.W. Hamming, *Numerical Methods for Scientists and Engineers*, **(**Dover Publications, 1987).
[52] E. Isaacson, and H.B. Keller, *Analysis of Numerical Methods*, **(**Dover Publications, 1994).
[53] F.B. Hildebrand, *Introduction to Numerical Analysis*, **(**Dover Publications, 1987).
[54] A. Greenbaum, and T.P. Chartier, *Numerical Methods: Design, Analysis, and Computer Implementation of Algorithms*. (Princeton University Press, 2012).
[55] A.J. Salgado, and S.M. Wise, *Classical Numerical Analysis: A Comprehensive Course.* **(**Cambridge University Press, 2023).
[56] D.E. Stewart, *Numerical Analysis: A Graduate Course*, (Springer; 2022).
[57] J.H. Mathews, and K.D. Fink, *Numerical Methods. Using Matlab*, third edition (Amazon, 1998).
[58] V.G. Rudychev, M.O. Azarenkov, I.O. Girka, V.T. Lazurik, and Y.V. Rudychev, Radiation Physics and Chemistry, **206**, 110815 (2023). https://doi.org/10.1016/j.radphyschem.2023.110815
[59] V.G. Rudychev, V.T. Lazurik, and Y.V. Rudychev, Radiation Physics and Chemistry, **186**, 109527 (2021). https://doi.org/10.1016/j.radphyschem.2021.109527
[60] V. Lazurik, S. Sawan, V. Lazurik, and O. Zolotukhin, in: *4th International Maghreb Meeting of the Conference on Sciences and Techniques of Automatic Control and Computer Engineering Proceedings*, (IEEE, Maghreb, 2024), pp. 649–653. https://doi.org/10.1109/MI-STA61267.2024.10599694
[61] G. Lewin, *Fundamentals of Vacuum Science and Technology*. (McGraw-Hill, 1965).
[62] J.M. Lafferty. *Foundations of Vacuum Science and Technology*. (John Wiley & Sons, 1998).

МОДЕЛЮВАННЯ ФОКУСУВАННЯ ПОРОЖНИСТОГО ЕЛЕКТРОННОГО ПУЧКА СИМЕТРИЧНОЮ МАГНІТНОЮ ЛІНЗОЮ ДЛЯ ПРОМИСЛОВОГО ЗАСТОСУВАННЯ В АДИТИВНИХ ТЕХНОЛОГІЯХ

Ігор В. Мельник[1], Сергій Б. Тугай[1], Михайло Ю. Скрипка[1], Микола С. Суржиков[1], Олександр М. Коваленко[1], Дмитро В. Ковальчук[2]

[1]Національний технічний університет України «Київський політехнічний інститут імені Ігоря Сікорського»
[2]Приватне акціонерне товариство «НВО «Червона Хвиля»

У статті, з використанням методів чисельного моделювання, досліджено особливості фокусування короткофокусного порожнистого пучка електронів, сформованого з широкої поверхні холодного катода в електронних гарматах високовольтного тліючого розряду. Для отримання відповідних результатів моделювання використано оригінальне програмне забезпечення, створене авторами на мові програмування Python. Аналіз отриманих результатів чисельного моделювання показав, що у разі невеликої зміни кута розбіжності траєкторії пучка або радіуса початкової точки на поверхні катода положення фокусу пучка, як правило, не змінюється. Тому кільцевий фокус пучка зазвичай займає стійке положення по поздовжній координаті, а товщина фокального кільця завжди знаходиться в межах кількох міліметрів. Відповідні теоретичні результати порівнювалися з експериментальними, та різниця між теоретичними та експериментальними результатами знаходиться в межах 10-15% залежно від прискорювальної напруги та розміру поверхні катода. Високовольтні електронні гармати тліючого розряду з такими параметрами за товщиною фокального кільця можуть бути успішно використані в прогресивних промислових адитивних технологіях тривимірного друку на металевих поверхнях шляхом рівномірного нагрівання за периметром рухомого дроту або стрижнів різного діаметра, в діапазон 0,5 – 10 мм.

Ключові слова: *Адитивні технології; Електронно-променеві технології, Магнітне фокусування, Порожнистий конусний електронний пучок, Числове моделювання*